Available online at www.sciencedirect.com

ScienceDirect

Radiology of Infectious Diseases 2 (2015) 162–167

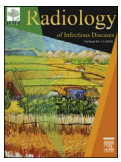

www.elsevier.com/locate/jrid

Research article

Integrated analysis of autoimmune pancreatitis by CT, MRCP and DWI

XinLong Pei, JingXia Xie*, JianYu Liu, Jing Su

Dept. of Radiology, Peking University Third Hospital, 49 North Garden Road, Haidian District, Beijing 100191, PR China

Received 12 May 2015; revised 11 July 2015; accepted 8 September 2015
Available online 1 December 2015

Abstract

Purpose: CT, MRCP and diffusion weighted imaging characteristics were discussed to improve the diagnostic accuracy of autoimmune pancreatitis.
Materials and methods: 23 cases of confirmed autoimmune pancreatitis were retrospectively analyzed before treatments. 23 cases underwent CT unenhanced and enhanced scans, 21 cases underwent MRCP examination, and 11 cases underwent DWI examination. Pancreatic lesion, involvement of the pancreatic duct and bile duct, changes of adjacent artery and vein, and other organs lesions. CT values and ADC values of pancreas and lesion were measured.
Results: Focal type lesions were shown in 6 cases, diffuse type in14 cases, and both types in 3 cases. Diffuse pancreatic swelling was shown in 20 cases, and peripancreatic halo in 13 cases. Mean CT values of lesions: unenhanced scan 35.81 ± 6.23 HU, late arterial phase 75.80 ± 17.47 HU, venous phase 93.19 ± 14.06 HU, and equilibrium phase 90.00 ± 14.67HU. Delayed homogenous enhancement was shown in 17 cases. Tapered narrowing (12 cases) or multiple segmental pancreatic duct stenosis (8 cases) was detected, the absence of main pancreatic duct dilatation or less than 3.5 mm in 20 cases, and duct penetrating sign in 20 cases. Bile duct lesions were found in 20 cases. ADC values of lesions ($0.99 \pm 0.03 \times 10^3$ mm^2/s) were significantly lower that of pancreas ($1.47 \pm 0.16 \times 10^3$ mm^2/s).
Conclusion: CT and MRI integrated diagnosis was helpful for accurate diagnosis based on the distinctive imaging characteristics of autoimmune pancreatitis.

Keywords: Autoimmune pancreatitis (AIP); Tomography; X-ray computed; Magnetic resonance imaging (MRI); Diffusion weighted imaging (DWI)

1. Introduction

Autoimmune pancreatitis (AIP) is a special type of chronic pancreatitis, with a incidence of 2%–11% [1,2]. AIP usually occurs in people more than 50 years old, with a male to female ratio of 3:1. The patients often present with jaundice, upper abdominal pain, weight loss, fat diarrhea, nausea, vomiting, etc, and acute onset of disease is rare. Etiology is still not clear and considered related to immune adjustment disorder. The diagnostic approach to AIP includes imaging, laboratory examination, histology, other organ involvement outside pancreas, reflection after steroid therapy [3,4]. Diagnosis specificity and sensitivity of serological indexes, such as IgG4 and IgG, remain controversial, because the indexes don't increase in some cases [3]. The specificity of the biopsy is not high, which belongs to invasive examination [5]. All diagnostic criteria consider imaging as critical examination. CT enhancement can evaluate the morphology and enhancement degree of pancreas and its surrounding tissues, MRI can provide a higher resolution of soft tissue, MRCP has some advantages in evaluating the pancreatic duct and bile duct, and DWI can provide histological information from view of molecular diffusion movement [6–8]. Integrated application of these inspection methods could promote the accurate diagnosis of the disease. Therefore, the purpose of this study is to investigate integrated diagnosis value for autoimmune pancreatitis (AIP) by dynamic enhanced CT, magnetic

* Corresponding author.
E-mail address: mrpxl@126.com (J. Xie).
Peer review under responsibility of Beijing You'an Hospital affiliated to Capital Medical University.

http://dx.doi.org/10.1016/j.jrid.2015.11.001

resonance cholangiopancreatography (MRCP) and diffusion weighted imaging (DWI).

2. Patients and methods

2.1. Subjects

According to international consensus of AIP diagnostic criteria of 2011 international association of pancreatic disease [3], 23 cases of the AIP patients were retrospectively analyzed since 2008. Among them, 6 cases were confirmed by surgery, 9 cases by endoscopic retrograde cholangiopancreatography (ERCP) and biopsy, 8 cases by review after steroid therapy. The study patients consisted of 3 women and 20 men (mean age 63.2 ± 15 years). The main symptoms included jaundice, abdominal pain, abdominal distention, diarrhea, angular, fatigue, fever, etc, of which 13 cases jaundice. IgG4 increased in 3 cases, IgG increased in 6 cases, and IgE increased in 6 patients.

2.2. CT and MRI parameters

23 cases were consecutively referred for unenhancement CT scan and late arterial (38−42 s) and venous phase (60−65 s) enhancement scanning, of which 13 cases for equilibrium phase (120 s−180 s) examination before treatment, with window width of 170 HU and window level of 35 HU. Spiral scan scope ranged from diaphragm to inferior margin of sacroiliac joint in 23 cases. At the same time, 3 cases went through thorax scan, 2 cases pelvis scan, and 1 case neck scan. CT scanner (Discovery HD 750, GE) was using, and parameters were as follows: slice thickness 3.5 mm, slice space 3.5 mm, careKV, detector width 64 * 2 * 0.6 mm, pitch 0.8, rotation speed 0.5 s. Contrast agent was non-ionic contrast agent (Ioversol 350 mgI/ml, tyco healthcare, the United States), 80 ml, injected with 3.0 ml/s by median cubital vein. After the whole scan, the venous phase images were reconstructed coronally, with slice thickness 3.5 mm and slice space 3.5 mm.

MRCP sequence was carried out for 21 cases AIP patients before treatment, of which 11 for DWI examination. MRI scanner was Siemens 3.0 T superconducting scanner (MAGNETOM TRIO TIM, Siemens, Erlangen, Germany), with b value of 0 s/mm^2, 500 s/mm^2, 1000 s/mm^2. Parameters are shown in Table 1.

2.3. Image analysis and measurements

CT, MRCP and DWI sequence images were respectively evaluated by two radiologists (12 years and 15 years CT and MRI working experience), coming to an agreement after discussion. The location, shape and range of the lesion were recorded. The enhancement degree and uniformity were observed in CT enhanced image. The shapes of pancreatic duct and bile duct were observed in MRCP images. At the same time, the shape of whole pancreas and the surrounding involvement, adjacent affected arteries and veins, and concomitant lesions in other viscera were also recorded. DWI features of AIP lesions and normal pancreatic tissues were compared.

The whole pancreas was divided into three parts: head, body and tail. The lesion, confined to one part as nodule, was defined as the focal type. The lesion, distributed in the two or more than two parts, was defined as the diffuse type. Lesion with the two above distribution was defined as the mixed type.

For focal AIP type, CT values of unenhancement and enhancement images and apparent diffusion coefficient (ADC) values of the lesions and normal pancreatic parenchyma were measured. For diffuse AIP type, CT values and ADC values of lesions were measured. Regions of interest (ROI) of lesion area were about 0.5−1 cm^2, and normal pancreatic parenchyma ROIs were about 0.2−0.5 cm^2. Fat tissue should be avoid for patients with pancreas atrophy or fatty infiltration. ADC values mean were calculated and compared between lesions and normal pancreatic parenchyma. The average CT value of lesions (unenhancement Du, late arterial phase Da, venous phase Dv, and equilibrium phase De) and the CT value ratio of lesion and normal pancreas (unenhancement Du/Pu, late arterial phase Da/Pa, venous phase Dv/Pv, and equilibrium phase De/Pe).

2.4. Pathology

Pathologic results were available for 6 patients by surgeries, and 9 patients by ERCP and biopsies. Pathologist (with 9 years of experience in pancreas and hepatobiliary pathology) reviewed the pathology slides and the macroscopic pictures of the resected specimen with no knowledge of the imaging findings. All surgery or biopsy specimens were fixed in 10% neutral buffered formalin for 6−48 h, embedded in paraffin, cut sections, and stained with hematoxylin-eosin (HE) for

Table 1
MRCP and DWI parameters.

	TR/TE (ms)	ETL	FA (°)	Section thickness (mm)	Slice gap (mm)	FOV (mm)	Matrix
T2 TSE	188/93	29	120	6	1.2	380	320*320
T1 FLASH-FS	174/2.46		70	5	1.0	350	320*256
Thick-section MRCP[a]	4500/751	307	180			320	512*307
Thin-section MRCP	1500/92 TI = 200 ms	256	150	4	0.4	340	320*256
DWI	2100/73			6	1.2	350	192*120

[a] Slab thickness 60 mm.

microscopic examination. In immunohistochemical staining, En Vision two footwork was used, including CD38, IgG, and IgG4.

2.5. Statistical analysis

Kappa test was used to evaluate the result consistency between two observers. The reference evaluation principle of the Kappa value (K value): <0.8 K $\leq$ 1.0, diagnostic consistency was wonderful; $0.4 <$ K ≤ 0.8, diagnostic consistency was good; $0 <$ K ≤ 0.4, diagnostic consistency was bad, Significant level for a $= 0.05$. Statistical significance was calculated using paired sample t test for CT value and ADC value comparisons, and $P < 0.05$ was chosen as statistically significant.

3. Results

23 AIP patients included focal type 6 cases (26.1%), diffuse type 14 cases (60.9%) and combination type 3 cases (13.0%) (Table 2). Focal type included 5 cases single lesion (2 in pancreatic head and 3 in body and tail) (Fig. 1) and 1 case multiple lesions. Diffuse type involved the whole pancreas (Fig. 2). Combination type (focal and diffuse type coexisting) involved the pancreatic head and body and tail (Fig. 3). CT performance include pancreas local swelling or diffuse enlargement as sausage, with uniform density, a low density halo around the gland. In MR images, the lesions and halo are shown slightly hyperintensity in T2WI and slightly hypointensity in T1WI. The lesions were showed most clearly in T1 FLASH-FS sequence compared with other MR sequences and CT images.

AIP lesions were shown homogeneous hypodensity in unhancement CT scan, and uniform enhancement in three phases images. In 17 (73.9%) cases, enhancement degree increased gradually (Fig. 1A–C), of which lesion CT values of 8 cases were close to normal pancreaes in equilibrium phase. For the other 6 cases (26.1%), enhancement degree did not increased. CT value statistics of AIP lesions and CT value ratio of lesion and normal pancreas were shown in Table 3.

21 cases MRCP performance: The pancreatic duct in part of AIP lesions, was shown a tapered stenosis in 12 cases (57.1%) (Fig. 1F), multiple segmental stenosis and skip distributed in 8 cases (38.1%) (Fig. 2E), and rough pancreatic duct without stenosis in 1 case. Pancreatic duct are visible through AIP lesion in 20 cases (95.2%), and only 1 case showed duct occlusion. Upstream pancreatic duct did not show dilation in 11 cases, mild dilation (less than 3.5 mm) in 9 cases, and obvious dilation (7 mm) in 1 case. The pancreas atrophy was not found in all cases. For 2 cases who only went through CT examination, pancreatic duct was not detected.

In 21 cases, 20 cases (95.2%) were accompanied with different degrees of extrahepatic bile duct lesions. 15 cases (71.4%) intrapancreatic portion of the common bile duct showed tapered stenosis (Fig. 1F), 2 cases showed truncation stenosis (Fig. 2E), 1 case showed rough bile duct wall, and 2 cases showed multiple strictures of common bile duct and hepatic portal bile duct. 19 cases (90.5%) showed secondary dilation of intrahepatic and extrahepatic bile duct, while 1 case did not show dilation bile duct. In 20 cases with bile duct lesion, 1 case with AIP lesion confined in the body, still was accompanied with bile duct wall thickening, luminal stenosis and secondary dilation. 2 cases with biliary drainage tube only went through the CT examination, so it was difficult to judge the stenosis degree of bile duct.

11 cases AIP lesions were shown slightly higher intensity than the pancreas (Fig. 1G), and average ADC values of lesions was $0.99 \pm 0.03 \times 103$ mm^2/s. Normal pancreas average ADC values was $1.47 \pm 0.16 \times 103$ mm^2/s. ADC of AIP lesions values were less than normal pancreatic tissue (Fig. 1H), with significant difference ($P < 0.001$).

In 23 cases, 3 cases involved multiple blood vessels, including pulmonary arteries, abdominal aorta, subclavian artery and inferior mesenteric artery, iliac artery, characterized by wall thickening and cavity expansion; 3 cases involved both kidneys, detected as multiple focal lesions with mild or moderate enhancement; 2 cases involved lymph nodes, including submandibular region, parotid gland, jugular vein region, supraclavicular, axillary, lung hilus, mediastinum, region of abdominal aorta and iliac blood vessels, and groin; 1 case appeared mesenteric effusion; and 1 case appeared submandibular gland enlargement.

15 cases pathological examination showed different degree of pancreatic ductal wall thickening, periductal lymphocytes and plasma cells infiltration with varying degree of fibrosis, and occlusive phlebitis. IgG4 positive plasma cell infiltration appeared in 3 cases.

4. Discussion

4.1. AIP lesion

Typical AIP was characterized by pancreas diffuse enlargement as sausage shape, uniform density, mild or moderate enhancement, and low density halo around pancrease [9]. The literature reported 57 cases AIP, diffuse (44%),

Table 2
Lesion morphology and vascular involvement in AIP.

(n = 23)	Lesion		Pancrease			Vascular involvement		
	Shape	Size (cm)	Sausage	Atrophy	Halo	Splenic artery	Splenic vein	Portal vein
Diffuse (n = 14)	Diffuse		14	no	8	3	8	
Focal (n = 6)	Nodule	1.7–3.3 (2.2 ± 0.7)	3	no	4	1	1	1
Combination (n = 3)			3	no	1		1	

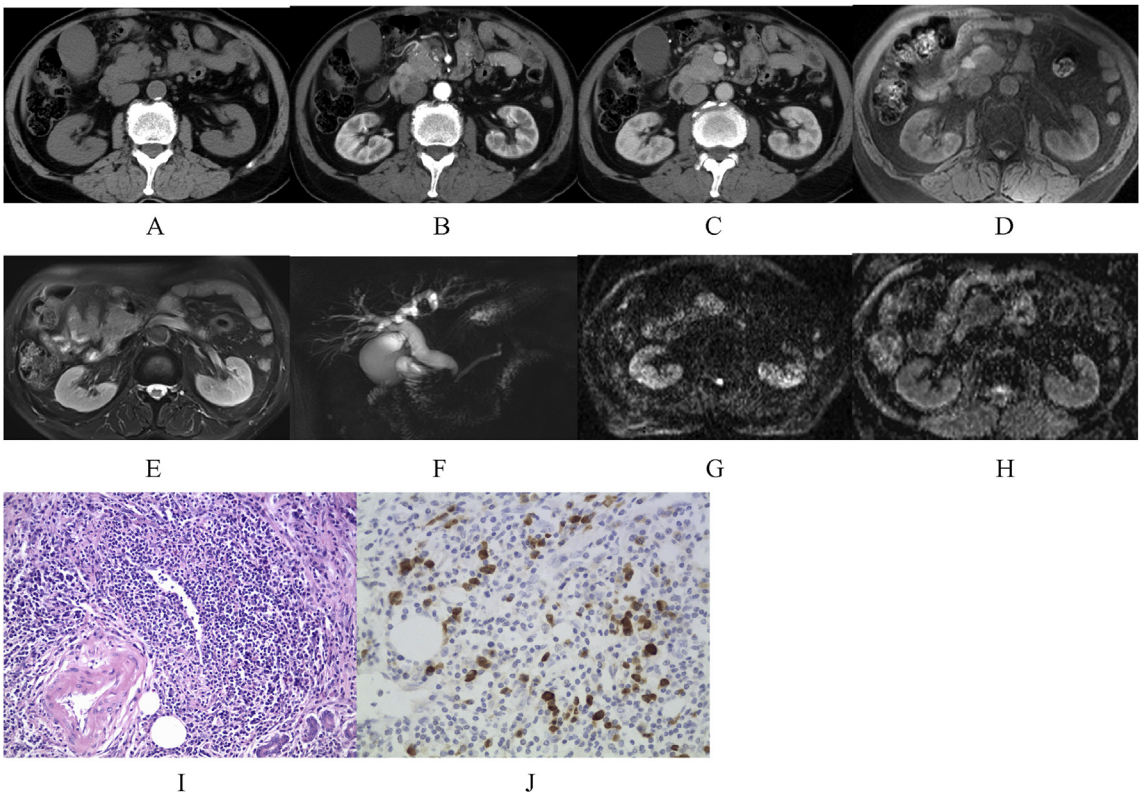

Fig. 1. M/75. Focal lesion in pancreatic head. Unhancement CT image (A) showed lightly low density, late arterial phase (B), venous phase (C) images showed enhanced uniformly and gradually. MR T1FS (D) showed slightly hypointensity in T1WI, and slightly hyperintensity in TSE FS T2WI (E). MRCP (F)showed narrowing of the pancreatic head duct and mild upstream pancreatic duct dilatation, and gradual stenosis of intrapancreatic portion of the common bile duct and obvious dilatation of intrahepatic and extrahepatic bile duct. DWI (G) showed slightly hyperintensity lesion, and ADC map (H) showed hypointensity. Hematoxylin-eosin [H−E] stain, original magnification, ×200 (I) showed thickening of the pancreatic duct wall, periductal inflammation associated with fibrosis, and obliterative phlebitis. IgG4 immunostain; original magnification, ×400 (J) shows IgG4-positive plasma cells around the pancreatic duct.

focal (49%), multiple focal 7% [10]. In our study, diffuse type, combination type and multiple focal were majority (78.3%, 18/23), while single focal type was minority (21.7%,5/23), that the difference may be associated with less number of cases. Pancreatic atrophy was not seen in AIP. Sausage shaped pancreas and halo sign were observed in the majority of cases, from the previous literature and our cases [11]. Because normal pancreatic tissue was characterized by high signal in

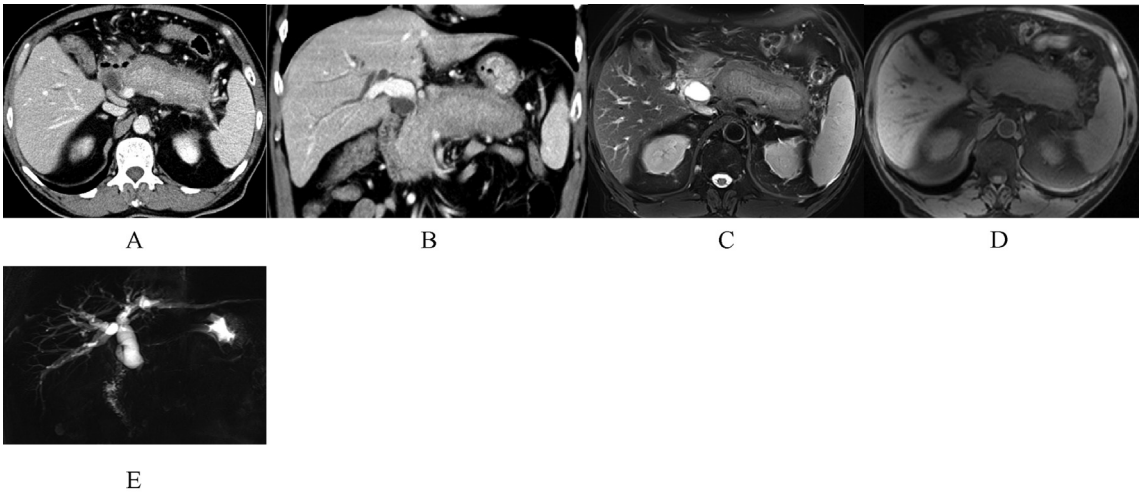

Fig. 2. M/63. Diffuse AIP. Venous phase CT image (A) showed diffuse enlargement, with a low density halo and stenosis of splenic vein. Venous phase coronal reconstruction (B) showed stenosis of intrapancreatic portion of the common bile duct and thickening of wall. MR T2WI TSE (C) and FS T1WI (D) images showed diffuse enlargement and a hypointensity halo. MRCP (E) showed multiple narrowing of pancreatic duct without upstream duct dilatation, and cutting stenosis of intrapancreatic portion of the common bile duct with obvious dilatation of intrahepatic and extrahepatic bile duct.

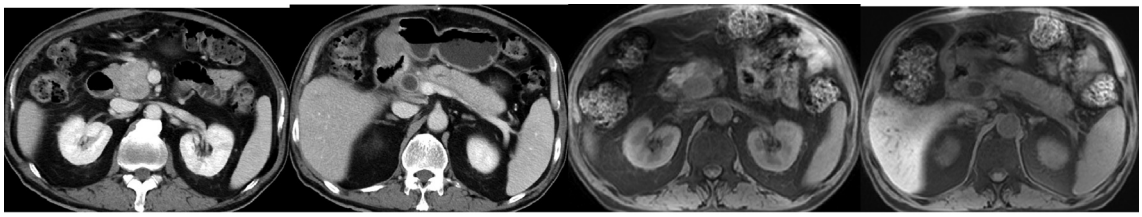

Fig. 3. M/63. Diffuse AIP in body and tail combined with focal lesion in head. Venous phase CT image showed uniform enhanced lesion in head (A) and diffuse enlargement in body and tail (B). MR FS T1WI showed lightly hypointensity lesions in head (C) and body and tail (D).

Table 3
CT value of AIP lesions and CT value ratio of lesion and normal pancreas[a].

	AIP	Normal pancreas	T	P
Unhancement	35.81 ± 6.23	41.23 ± 6.65	−2.454	0.020
Late arterial phase	75.80 ± 17.47	97.99 ± 6.04	−3.224	0.003
Venous phase	93.19 ± 14.06	103.24 ± 15.38	−2.100	0.043
Equilibrium phase	90.00 ± 14.67	95.56 ± 5.73	−0.758	>0.05

[a] For the case that lesion involved the whole pancrease, normal pancreatic tissue CT value did not be measured.

MR T1WI fat suppression sequence images, so the contrast between pancrease and AIP lesions was more prominent in the sequence, compared with unhancement CT scan images.

AIP lesions were characterized by uniform and low density in three enhancement phases, and most AIP lesions were enhanced obviously in venous phase and equilibrium phase, even close to the pancreas tissue density. This sign may be due to lymphocytes and plasma cells diffuse infiltration and fibrous tissue hyperplasia leading to slow contrast dispersion, and occlusive phlebitis restricting contrast agent elimination [12].

In this study, 47.8% (11/23) cases involved blood vessels, such as the splenic artery and vein and portal vein, and did not involved the superior mesenteric artery and pancreaticoduodenal artery. These cases mainly were diffuse type lesions, so it was concluded that blood vessels involving may be related to the location and larger scope of the diffuse lesions.

4.2. Involved pancreatic duct and bile duct

CT enhancement images can display the expansion of the pancreatic duct and bile duct, and scope and enhancement degree of thickening bile duct wall. MRCP was more sensitive than CT in showing the pancreatic duct and bile duct, especially for mild expansion or normal diameter duct [12,13]. In our most cases, the main pancreatic ducts were tapered or multiple segments narrowing, and upstream pancreatic duct expansion appeared less (47.6%, 10/21), even in cases with the pancreatic duct expansion, the expansion degree of most were less than 3.5 mm. Many literatures considered that the main pancreatic duct multiple irregular stenosis without the expansion of the upstream pancreatic duct (<5 mm)is one of the characteristics of AIP [11–16]. At the same time, pancreatic duct penetrating sign shown in our vast majority of cases, was considered as one of characteristics of the AIP [15], with sensitivity 73% and specificity 96%.

Bile ducts is the most common AIP involvement location except pancreas [17], especially lower part of bile duct. peripheral lymphocyte and plasma cell infiltration and fibrous tissue hyperplasia induced bile duct wall thickening and slender centrality narrow of duct lumen. In our study, 87.0% (20/23) cases involved common bile duct, consistent with literature reports. Besides, 1 case of focal lesion far from pancreatic head still was companied with common bile duct involvement, and 2 cases showed multiple segments stenosis of bile duct, which probably was significantly for the diagnosis of AIP.

4.3. DWI

In this study, ADC values of AIP lesions were significantly less than the normal pancreatic tissue [18,19], that was consistent with previous literature. Its pathological basis was still not clear, and was considered associated with the following factors: increase of cell components such as lymphocytes and plasma cells, and fiber tissue hyperplasia, made water molecules diffusion limited. ADC values had higher accuracy for AIP diagnosis. The optimal ADC cutoff value was 0.88 * 10-3 mm^2/s to distinguish AIP from pancreatic cancer, with the sensitivity of 100%, specificity of 89% [18]. ADC values varied slightly in different literatures, that may be related to some factors, such as the MRI scanner type, field strength, choice of b value, and the type of DWI sequence, et al. Higher b value should be chosen to reduce the T2 shining effect, perfusion effect, and background tissue signal [19].

4.4. Extrapancreatic lesions

In previous literatures, extrapancreatic involvements include: bile duct (77%), renal (35%), lymph nodes (33%), gall bladder (16%), retroperitoneal and mesenteric, thyroid, lacrimal gland, orbit, salivary gland, lung, gastrointestinal tract, and blood vessels, et al. [20–23]. Its pathological basis was uniform to pancreas AIP. Our cases involved blood vessels, kidneys, lymph nodes, mesenteric, submandibular gland. The less involvement organs may be associated with less cases of this group. These signs were of great help for the differential diagnosis of AIP.

4.5. Differential diagnosis

Due to the pancreatic duct and bile duct stenosis and secondary upstream duct dilation in most of AIP cases, especially focal lesions, so these often were distinguished from pancreatic ductal adenocarcinoma. The following points were helpful [12,18]: (1) typical pancreatic cancer usually was shown as nodular, with secondary upstream pancreatic duct dilation (>5 mm) and pancreatic parenchyma atrophy. (2) involved common bile ducts often were shown as truncated narrowing, and lesions in body or tail did not affect the bile duct. (3) pancreatic cancer frequently oppressed or invaded adjacent organs, such as duodenum, stomach, and blood vessels, with intraperitoneal or retroperitoneal lymph node metastasis, and metastasis of distant organs, such as liver, lung et al., in late stage.

5. Conclusion

In conclusion, the imaging findings of AIP were complicated, including pancreas swelling like sausage shape, with circumambient halo and delay enhancement in portal venous or equilibrium phase, without obvious upstream pancreatic duct dilation. ADC value of AIP was significantly less than pancreas, often accompanied by lesions of other organs. Fully understanding these signs and choosing the appropriate examination way had a high clinical value for correct diagnosis.

References

[1] Chari ST, Kloeppel G, Zhang L, Notohara K, Lerch MM, Shimosegawa T. Histopathologic and clinical subtypes of autoimmune pancreatitis: the Honolulu consensus document. Pancreatology 2010;10:664−72.

[2] Shanbhogue AK, Fasih N, Surabhi VR, Doherty GP, Shanbhogue DK, Sethi SK. A clinical and radiologic review of uncommon types and causes of pancreatitis. Radio Graph 2009;29(4):1003−26.

[3] Shimosegawa T, Chari ST, Frulloni L, Kamisawa T, Kawa S, Mino-Kenudson M, et al. International consensus diagnostic criteria for autoimmune pancreatitis: guidelines of the International Association of Pancreatology. Pancreas 2011;40(3):352−8.

[4] Khandelwal A, Shanbhogue AK, Takahashi N, Sandrasegaran K, Prasad SR. Recent advances in the diagnosis and management of autoimmune pancreatitis. Am J Roentgenol 2014;202(5):1007−21.

[5] Bang SJ, Kim MH, Kim DH, Lee TY, Kwon S, Oh HC, et al. Is pancreatic core biopsy sufficient to diagnose autoimmune chronic pancreatitis? Pancreas 2008;36:84−9.

[6] Do RK, Katz SS, Gollub MJ, Li J, LaFemina J, Zabor EC, et al. Interobserver agreement for detection of malignant features of intraductal papillary mucinous neoplasms of the pancreas on MDCT. Am J Roentgenol 2014;203(5):973−9.

[7] Kim SH, Lee JM, Lee ES, Baek JH, Kim JH, Han JK, et al. Intraductal papillary mucinous neoplasms of the pancreas: evaluation of malignant potential and surgical resectability by using MR imaging with MR cholangiography. Radiology 2015;274(3):723−33.

[8] Jang KM, Kim SH, Kim YK, Park MJ, Lee MH, Hwang J, et al. Imaging features of small (≤ 3 cm) pancreatic solid tumors on gadoxetic-acid-enhanced MR imaging and diffusion-weighted imaging: an initial experience. Magn Reson Imaging 2012;30(7):916−25.

[9] Sah RP, Chari ST. Autoimmune pancreatitis: an update on classification, diagnosis, natural history and management. Curr Gastroenterol Rep 2012;14:95−105.

[10] Kim KP, Kim MH, Kim JC, Lee SS, Seo DW, Lee SK. Diagnostic criteria for autoimmune chronic pancreatitis revisited. World J Gastroenterol 2006;12(16):2487−96.

[11] Vlachou PA, Khalili K, Jang HJ, Fischer S, Hirschfield GM, Kim TK. IgG4-related sclerosing disease: autoimmune pancreatitis and extrapancreatic manifestations. Radio Graph 2011;31:1379−402.

[12] Wang J, Su T, Jia N, Wang J, Wang C, Wang S, et al. Computed tomographic and magnetic resonance imaging presentations of pancreatitis maldiagnosed as pancreatic carcinoma. Pancreas 2010;39:262−4.

[13] Manfredi R, Frulloni L, Mantovani W, Bonatti M, Graziani R, Pozzi Mucelli R. Autoimmune pancreatitis: pancreatic and extrapancreatic MR imaging-MR cholangiopancreatography findings at diagnosis, after steroid therapy, and at recurrence. Radiology 2011;260:428−36.

[14] Carbognin G, Girardi V, Biasiutti C, Camera L, Manfredi R, Frulloni L, et al. Autoimmune pancreatitis: imaging findings on contrast-enhanced MR, MRCP and dynamic secretin-enhanced MRCP. Radiol Med (Torino) 2009;114(8):1214−31.

[15] Hur BY, Lee JM, Lee JE, Park JY, Kim SJ, Joo I, et al. Magnetic resonance imaging findings of the mass-forming type of autoimmune pancreatitis: comparison with pancreatic adenocarcinoma. J Magn Reson Imaging 2012;36:188−97.

[16] Shin JU, Lee JK, Kim KM, Lee KH, Lee KT, Kim YK, et al. The differentiation of autoimmune pancreatitis and pancreatic cancer using imaging findings. Hepatogastroenterology 2013;60(125):1174−81.

[17] Kamisawa T, Takuma K, Anjiki H, Egawa N, Kurata M, Honda G, et al. Biliary lesions associated with autoimmune pancreatitis. Hepatogastroenterology 2009;56(93):1190−3.

[18] Muhi A, Ichikawa T, Motosugi U, Sou H, Sano K, Tsukamoto T, et al. Mass-forming autoimmune pancreatitis and pancreatic carcinoma: differential diagnosis on the basis of computed tomography and magnetic resonance cholangiopancreatography, and diffusion-weighted imaging findings. Magn Reson Imaging 2012;35:827−36.

[19] Kamisawa T, Takuma K, Anjiki H, Egawa N, Hata T, Kurata M, et al. Differentiation of autoimmune pancreatitis from pancreatic cancer by diffusion-weighted MRI. Am J Gastroenterol 2010;105(8):1870−5.

[20] Chiba K, Kamisawa T, Kuruma S, Iwasaki S, Tabata T, Koizumi S, et al. Major and minor duodenal papillae in autoimmune pancreatitis. Pancreas 2014;43(8):1299−302.

[21] Kamisawa T, Takuma K, Kuruma S, Fujiwara J, Anjiki H, Koizumi K, et al. Lacrimal gland function in autoimmune pancreatitis. Intern Med 2009;48(12):939−43.

[22] Kasashima S, Zen Y, Kawashima A, Endo M, Matsumoto Y, Kasashima F. A new clinicopathological entity of IgG4-related inflammatory abdominal aortic aneurysm. J Vasc Surg 2009;49(5):1264−71.

[23] Fujinaga Y, Kadoya M, Kawa S, Hamano H, Ueda K, Momose M, et al. Characteristic findings in images of extra-pancreatic lesions associated with autoimmune pancreatitis. Eur J Radiol 2010;76(2):228−38.